On the first step in zinc deposition – A case of nonlinear coupling with the solvent

Paola Quaino [a], Estefania Colombo [a], Fernanda Juarez [b], Elizabeth Santos [b], Gustavo Belletti [a], Axel Groß [b,c], Wolfgang Schmickler [b,*]

[a] Instituto de Química Aplicada del Litoral, IQAL (UNL-CONICET), Santa Fe, Argentina
[b] Institute of Theoretical Chemistry, Ulm University, Germany
[c] Helmholtz Institute Ulm (HIU), Germany

ARTICLE INFO

ABSTRACT

The deposition of zinc from aqueous solutions is of great practical importance, and it also serves as a prototype for the deposition of divalent ions. Both experiment and theory agree, that it takes place in two steps. Previous theoretical work [1] had suggested that the step, $Zn^{++} + e^- \rightarrow Zn^+$ takes place in the outer sphere, but gave a prohibitively high energy of activation of the order of 1.4 eV, in accord with the enigma of metal deposition postulated by Gileadi [2]. In this work the treatment of the reactant – solvent interaction is substantially improved by introducing nonlinear terms based on molecular dynamics. Our calculations suggest that the first steps follows an inner sphere path with a much lower energy of activation, which results in a physically adsorbed Zn^+ ion. The second step then occurs on the electrode surface. These findings are in line with experimental data.

1. Introduction

Zinc deposition and dissolution has a long and illustrious history in electrochemistry. It started with the famous pile of Volta, who used zinc as one of the electrode materials, and for a long time the Leclanché cell, based on zinc and manganese, was the most common type of battery.

During the last decades, Zn deposition on Zn metal anodes has raised quite some interest due to the fact that it is a crucial process in Zn-air batteries [3,4]. Metal-air batteries in general promise very high energy densities. In addition, Zn is globally abundant which makes it an inexpensive and sustainable resource. And indeed, Zn-air batteries are already successfully commercialized, in particular as hearing aid batteries [5]. However, these commercial batteries are only available as primary batteries. The utilization of rechargable Zn-air batteries is hampered by the fact that their operation is plagued by dendrite growth at the Zn metal anode [3,4]. There are promising approaches to circumvent this dendrite growth. However, there are still some open questions left with respect to the deposition at battery metal anodes [6], which makes a better understanding of zinc deposition and dissolution not only scientifically interesting but also technologically relevant.

Besides these practical applications the zinc electrode poses interesting problems for fundamental electrochemistry. It is one of the prime examples of what Gileadi [2] called the enigma of metal deposition. With a hydration energy of the order of 20 eV, how can divalent metal ions ever shed their hydration shells and be deposited on an electrode surface? A few years ago, Pinto and a few of the authors of this paper [1] examined the deposition of Cu^{++} and of Zn^{++} on the basis of the theory proposed by Santos and Schmickler [7,8] and concluded, that these reactions take place in two steps: first an outer sphere electron transfer to the divalent ion, and then the monovalent ion is deposited onto the metal surface. For copper the outer sphere step is quite favorable, since the Cu^+ ion is almost stable in aqueous solutions, and the results for copper deposition compared quite well with experimental results. However, the Zn^+ ion has a very high energy, and the calculations predicted an excessively high activation energy of the order of 1.4 eV, which is in accord with Marcus theory [9]. The authors concluded that copper deposition can be understood in terms of theory, but the enigma of zinc deposition remained.

Obviously, something was missing in the model. At the outset of the present investigations we thought that the neglect of the image interaction of the Zn^{++} with the metal surface was the problem. Indeed, in earlier models, based on simple estimates rather than on density functional theory (DFT) and molecular dynamics, image interactions played an important role in attracting the ion to the surface [10]. However,

---

molecular dynamics simulations, which we shall report below, show that in the important region where the Zn^{++} loses its solvation shell, the image interaction is almost totally shielded by the surrounding water.

Instead we found the solution to the problem in another effect: As is common in the theory of electron transfer reactions the authors of [1] had assumed a linear coupling between the reactants and the solvent. While this approximation works reasonably well far from the surface, it breaks down in the region where the divalent ion starts to lose its solvation shell. Therefore we have included nonlinear terms into the model, and obtained the corresponding parameters from molecular dynamics. Our new calculations suggest a much more favorable pathway, in which the first electron transfer to the Zn^{++} ion occurs in an inner sphere mode and results in a Zn^+ ion which is physisorbed on the surface. The second step, the deposition onto the terrace, takes place directly on the surface.

In essence, we believe that we have solved the enigma of zinc deposition. Note that our model does not contain adjustable parameters, but is based on results of DFT and molecular dynamics.

2. The model Hamiltonian

We consider the transfer of one electron, $Zn^{++} + e^- \rightarrow Zn^+$, from a zinc electrode. As in our previous work [1] we base our model on a Hamiltonian, whose parameters are obtained from density functional theory (DFT) and molecular dynamics. The valence orbital, labelled a, of the zinc atom can take up two electrons, and therefore we had previously considered a Hamiltonian with two spin states. However, the spin repulsion parameter U was found to be of the order of 8 eV, so that in Zn^+ only one spin orbital was occupied. This is in line with the fact, that this ion, in contrast to the Zn atom, is not chemically adsorbed on the zinc surface. Therefore we consider just one electronic state on the atom, which simplifies the calculations.

Therefore we employ a spinless version of the Anderson-Newns model [11,12] for the reactant and its interaction with a metal electrode:

$$H_{el} = \epsilon_a n_a + \sum_k \epsilon_k n_k + \sum_k \left[V_k c_k^+ c_a + V_k^* c_a^+ c_k \right] \tag{1}$$

The first two terms denote the reactant and the metal, the last term effects electron exchange between the metal and the reactant with amplitudes V_k. ϵ_k denotes the electronic energy of the metal states, n_k their number operator, and c_k^+ and c_k the creation and annihilation operators. The corresponding quantities for the state a are ϵ_a, n_a, c_a^+ and c_a. All energies ϵ_a and ϵ_k are measured with respect to the Fermi level of the metal.

Electron transfer is coupled to the reorganization of the solvent – we note in passing, that the reorganization of the ionic atmosphere has a negligible effect on electron transfer [13]. Just like in Marcus [9] and Hush [14] theory, the solvent modes are divided into a fast part, which is supposed to follow the electron transfer instantly, and a slow part, whose reorganization triggers the electron transfer. In the absence of quantum modes, the slow modes of the solvent can be represented by a single effective solvent coordinate q [7,15]. Usually it is assumed, that both modes couple linearly to the solvent. However, a linear coupling predicts that the solvation energy of the ions is proportional to the square of the charge. Textbooks suggest a value for the free energy of solvation of Zn^{++} of $\Delta G_{sol}(Zn^{++}) = -21.28$ eV [16]. For the monovalent ion no experimental data are available, so we estimated the value from molecular dynamics and obtained a value of $\Delta G_{sol}(Zn^+) = -5.69$ eV. These are bulk values, but the deviation from linear coupling becomes much worse when the ions approach the electrode surface. This can be seen in Fig. 1, which shows the solvation energy of Zn^+ and one quarter of the solvation energy of Zn^{++} as a function of the distance d from the surface as derived from molecular dynamics. In a linear theory the two curves would coincide. However, due to the stronger solvation of the Zn^{++} ion, its solvation energy becomes higher (less favorable) when its
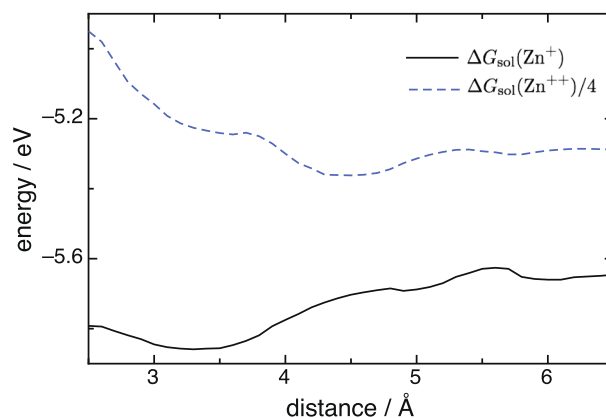

Fig. 1. Free energy of solvation $\Delta G_{sol}(Zn^+)$ for the univalent ion and $\Delta G_{sol}(Zn^{++})/4$ for the divalent ion as a function of the distance from the electrode surface. In a linear theory, both curves would coincide.

secondary solvation shell breaks up near $d \approx 4$ Å. Both curves have minima which are a little lower than the bulk values: For Zn^{++} the minimum is near $d = 4.5$ Å, where the secondary solvation shell is still intact, while for Zn^+ it is closer to the surface, near $d = 3.4$ Å. The reasons for this behavior have been discussed in detail in our previous work [1].

So we have to consider different reactant-solvent couplings for the two ions. The problem is similar to electron transfer involving frequency change as treated by Schmickler and Koper [17]. Following their example, we write the coupling terms as:

$$H_s = n_a \left[\lambda_1 q^2 + 2\lambda_1 q \right] + (1 - n_a)\left[\lambda_2 q^2 + 4\lambda_2 q \right] \tag{2}$$

The case $<n_a> = 1$ corresponds to the Zn^+ ion with energy of reorganization λ_1, while $<n_a> = 0$ corresponds to the Zn^{++} ion with energy of reorganization λ_2. For $\lambda_1 = \lambda_2 = \lambda$ these terms reduce to the familiar form: $\lambda q^2 + (z - n_a)2\lambda q$ [1,15], where $z = 2$ is the charge number of the ion core.

Finally, we specify the interaction with the fast solvent terms, which shift the electronic energies [15]. Thus, they give rise to the terms:

$$H_f = -n_a \lambda_1^f - 4(1 - n_a)\lambda_2^f \tag{3}$$

where λ_1^f and λ_2^f denote the coupling energies of the Zn^+ and Zn^{++} ions, resp., to the fast modes.

Within this model,:

$$\Delta G_{sol}(Zn^+) = -\lambda_1 - \lambda_1^f \qquad \Delta G_{sol}(Zn^{++}) = -4\lambda_2 - 4\lambda_2^f \tag{4}$$

which explains, why we introduced the factor four in the second part of Eq. (3).

If the solvent is modeled as a dielectric continuum, the energy of reorganization is related to the solvation energy through.the so-called Pekar factor [18,19]:

$$P = \left(\frac{1}{\epsilon_s} - \frac{1}{\epsilon_\infty} \right) \approx 1/2 \quad \text{for water} \tag{5}$$

where ϵ_s is the static and ϵ_∞ the optical dielectric constant of the solvent. Therefore we set:

$$\lambda_1 = \lambda_1^f = |\Delta G_{solv}(Zn^+)|/2 \quad \lambda_2 = \lambda_2^f = |\Delta G_{solv}(Zn^{++})|/8 \tag{6}$$

A comparison with Eq. (4) shows that these definitions give the correct energies of solvation.

Our model Hamiltonian is the sum $H = H_{el} + H_s + H_f$. It is convenient to collect the terms in n_a:

$$\widetilde{\epsilon}_a n_a = \left[\epsilon_a + q^2(\lambda_1 - \lambda_2) + 2q(\lambda_1 - 2\lambda_2) + 4\lambda_2^f - \lambda_1^f \right] n_a \tag{7}$$

This shows that the fast solvent terms simply shift the energy, while the slow solvent terms enter via the solvent coordinate q.

Once the Hamiltonian is defined, the calculations proceed as in our previous works [1,8]. We summarize the relevant equations in order to make this article self-contained. The interaction of the reactant's level a with the metal gives rise to the two chemisorption functions:

$$\Lambda(x) = \mathscr{P}\sum_k \frac{|V_k|^2}{x - \epsilon_k} \qquad \Delta(x) = \pi\sum_k |V_k|^2 \delta(x - \epsilon_k) \qquad (8)$$

where x is the energy variable. They determine the density of states (DOS) of the reactant:

$$\rho(x) = \frac{1}{\pi}\ \frac{\Delta(x)}{(x - \widetilde{\epsilon}_a - \Lambda(x))^2 + \Delta(x)^2} \qquad (9)$$

The Zn ions interact only with the sp band of zinc. The coupling constants have been determined in Ref. [1], as has been the energy ϵ_a; note that all these quantities are a function of the distance d. The total energy of the system is then given by:

$$E(d, q) = \int_{-\infty}^{0} x\,\rho(x)dx + \lambda_2 q^2 + 4\lambda_2 q - 4\lambda_2 \qquad (10)$$

If we set $\lambda_1 = \lambda_2 = 0$ the Hamiltonian corresponds to adsorption from the gas phase. In order to validate our parameterization of the Anderson-Newns Hamiltonian, we also calculated the approach of Zn and the Zn^+ ion from the vacuum towards the surface also by DFT [1], and compared it with the Anderson-Newns results. At all distances the differences were well below 0.1 eV, so that no correction was required. Our model contains no adjustable parameters. The electronic interactions enter via the two chemisorption functions Δ and Λ, both of which depend on the distance. Our procedure to determine them has been detailed in [8,1]. The energies of hydration of the ions, as a function of distance, have been determined from molecular dynamics, and from these both the slow and the fast part of the solvation energy can be determined on the basis of Eq. (6). Obviously, our formalism can be applied equally well to the deposition of other divalent ions.

3. Results and discussion

Before presenting the free energy surface for the reaction, we briefly discuss the role of image interactions. The potentials of mean force for the zinc ions were calculated without accounting for image interactions. For the Zn^+ ion this should be no problem, because they are contained in the DFT calculations for the approach of the ion towards the surface. However, for the divalent ions they could be important. In fact, we expect a competition between solvation, which would like to keep the ion in the bulk, and the image force, which attracts it to the surface. Both interactions scale with the square of the charge. Recently Geada et al. [20] have developed an ingenious method to represent image interactions in classical molecular dynamics by polarizable atoms of the substrate. This method requires a parameterization for each metal substrate; unfortunately those for zinc are not available, but for copper they are. Fortunately Zn^{++} and Cu^{++} have very similar ionic radii of about $0.6 - 0.7$ Å, so we expect a similar behavior. Actually, for a classical metal the image interactions are independent of the nature of the metal. To investigate the effect of image interactions on these divalent ions, we have calculated the potentials of mean force (pmf) for the approach of Zn^{++} and Cu^{++} to a Cu(100) surface.

The results are shown in Fig. 2. As expected, the curves for both ions are very similar, more importantly, the inclusion of image interactions has a very small effect. The only notable feature is a small shift in the shoulder near 3 Å, which is slightly more favorable when images are considered. So the solvation effects are much more important than the image interactions. The latter are shielded by the surrounding water, and their neglect should have a negligible effect on our calculated free
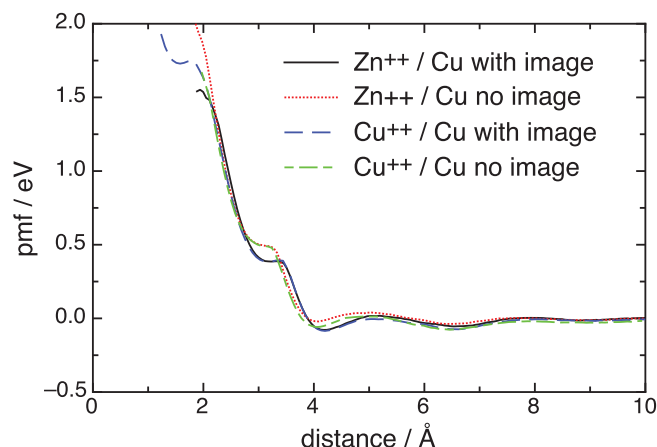

Fig. 2. Potentials of mean force for the approach of Cu^{++} and Zn^{++} towards a Cu(100) surface, calculated with and without image interactions.

energy surfaces.

First we examine the reaction at large distances, in the region where outer sphere electron transfer takes place. In this region, the interaction is weak, and the density of states can be replaced by a delta function $\delta(\widetilde{\epsilon}_a)$. The Zn^{++} state then corresponds to:

$$Zn^{++}: \quad < n_a > = 0, \quad q = -2, \quad \text{energy} = -8\lambda_2 = \Delta G_{\text{sol}}(Zn^{++}) \qquad (11)$$

and Zn^+ to:

$$Zn^+: \quad < n_a > = 1, \quad q = -1, \quad \text{energy} = \epsilon_a - 2\lambda_1 = \epsilon_a + \Delta G_{\text{sol}}(Zn^+) \qquad (12)$$

where the solvation and reorganization energies take their bulk values. Equilibrium in the outer sphere corresponds to:

$$\epsilon_a + \Delta G_{\text{sol}}(Zn^+) = \Delta G_{\text{sol}}(Zn^{++}) \qquad (13)$$

when the difference in the solvation energies is matched by the electronic energy. However, we are interested in the situation where Zn^{++} is in equilibrium with the zinc surface. An appropriate Born–Haber cycle shows that in this case the first step $Zn^{++} + e^- \rightarrow Zn^+$ is endergonic by about $\Delta G \approx 1.26$ eV. Therefore, in the calculations reported below we have increased the value of ϵ_a at large distances by this amount, i.e. the curve for ϵ_a as a function of the distance, as obtained from DFT, was shifted so that it attained its correct value at infinity.

We have recalculated the free energy surface for the deposition of zinc on Zn(0001) and included the nonlinear coupling. The electronic interactions and the potentials of mean force have been taken from [1]. The results are shown in Fig. 3 on the left hand side; this surface has been calculated for the case where the Zn^{++} ion is in equilibrium with Zn atoms at a kink site of the electrode surface. In the following, all energies are referred to that of the initial and final state. In the upper left corner, near $q = -2$ and $d = 4.5$, there is a distinct minimum corresponding to the Zn^{++} ion. The energy is even a little lower than the bulk value, which we have set to zero, because of the local minimum in the energy of solvation shown on Fig. 1. At the upper right corner, the energy takes the value of $\Delta G \approx 1.26$ eV by construction. At $d = 2.5$ Å and $q = -1$ there is a distinct minimum corresponding to a physisorbed Zn^+ ion with an energy of about 0.4 eV, which is substantially lower than the energy of the ion at large distances. This lowering of the energy is mainly caused by the electronic interaction with the zinc electrode [1], and the fact that the solvation energy at the surface is lower than the bulk value (see. Fig. 1). The two minima on the surface are separated by a saddle point with an energy of 0.9 eV, much lower than the value of energy of activation of about 1.44 eV reported in [1]. More importantly, there is a reaction path that leads directly from the Zn^{++} ion in the bulk to the
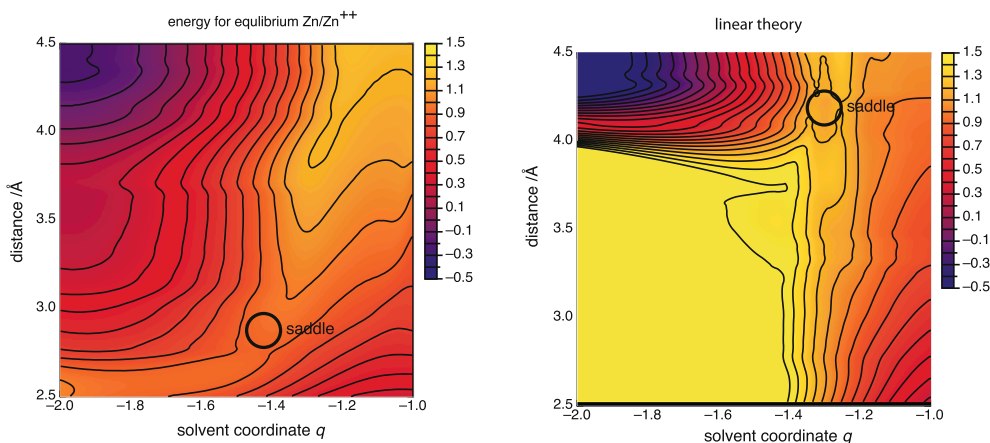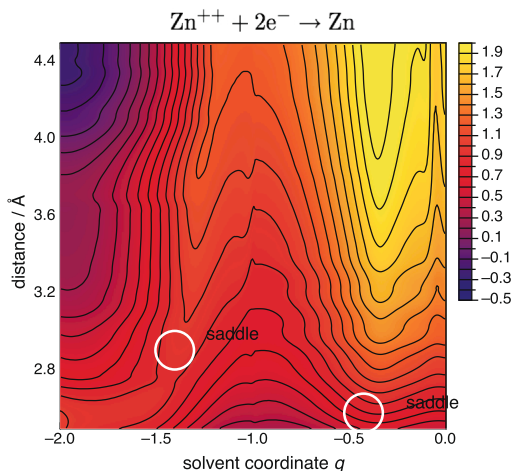
Fig. 3. Free energy surface for the reaction $Zn^{++} + e^- \rightarrow Zn^+$ at the equilibrium potential for the total reaction $Zn^{++} + 2e^- \rightarrow Zn$. Left: present nonlinear theory, right: results from the linear theory of Ref. [1].

physisorbed Zn^+ at the surface.

For comparison, we have replotted the corresponding surface from [1] on the right hand side of Fig. 3. In these older calculations, the average of the two energies of reorganization had been taken. Although this average value differs only by a few tenths of an eV from the values of λ_1 and λ_2, it has a significant effect because multiples of the reorganization energy enter into our equations. As a consequence, the energy of reorganization is too high in the lower left region; this entails an elevated energy, so that this region is blocked. Therefore, on the old surface the access to the minimum for Zn^+ at the surface was via the outer sphere path.

Using the same formalism as for the first step, we have calculated the reaction surface for the second step $Zn^+ + e^- \rightarrow Zn$ and joint it to the first surface – see Fig. 4. The saddle point for the second step is practically in the same position as in our previous work, but the activation energy has been lowered to about 0.6 eV. The absolute values of the activation energies obtained are not so precise because of the inherent difficulties of the calculations: (1) The solvation energies involved are high (-5.69 eV for Zn^+ and -21.28 for Zn^{++}), so that even small relative errors may have a noticeable effect. (2) The solvation energies for Zn^+ have been obtained from molecular dynamics based on a force field [1], and cannot be checked against experimental data. Therefore, the important result of our calculations is the reaction path, which differs essentially from that suggested in the previous work. According to our present work the first step does not take place in the outer sphere, where

independently of the details of the model it would encounter a prohibitively high activation energy, but in an inner sphere mode where the product is a Zn^+ ion physisorbed on the zinc surface. According to our calculation the energy of this metastable state is about 0.4 eV, but as mentioned above the absolute values have to be taken with a grain of salt. From this position the univalent ion is deposited onto the terrace of the surface, where its energy is about 0.35 eV with respect to the final state, where the atom sits at a kink site. The migration from the terrace to the kink is very fast only hindered by a rather small activation energy of 10 meV [6].

Zinc deposition and dissolution has been the subject of a fair number of studies. Early theoretical work, performed before the advent of DFT, suffered from the lack of reliable data for the electronic interactions between reactant and the electrode [22,10,21], but they all agreed that the reaction takes place in a series of two one-electron transfer steps. More recent DFT-based work by Rossmeisl et al. [23] is focused on alkaline solutions, where the zinc ions are complexed by OH, and the mechanism is quite different and cannot be compared with our work.

Experimental results are complicated by the fact that the mechanism of zinc deposition does not only depend on pH, but also on the kind of anions present in the solution. Early work used liquid electrodes, in particular mercury [24,25], or various amalgams [26]. They usually agree that the reaction takes place in two steps, and that the first step is rate-determining. Of course, experiments on amalgams cannot be directly compared with deposition on single crystal zinc, which we consider. However, they have the distinct advantage that the electrode surface is well defined. Experiments on zinc are more problematic; for a start, it is difficult to prepare a clean zinc surface. Most of the relevant work is cited in the very recent article by Zampardi and Compton [27]. Interestingly, several authors report the formation of an intermediate state consisting of complexed ions on the electrode surface – see [28] and references therein. Within our model, this could be interpreted in terms of a mechanism where the intermediate Zn^+ ion is stabilized by complexation. In the same vein, Zampardi and Compton postulate an reactant-like transition state, which is consistent with a rate-determining partial de-hydration/de-complexation process, which could perhaps be identified with our monovalent intermediate. These authors also report an unusually fast reaction with a rate constant of the order of 2 cm s^{-1}, as fast as the fastest outer sphere electron transfer reaction that have been measured in electrochemistry [7]. Perhaps the explanation lies in the nature of the method employed, the electrode-particle collision technique, in which nanoparticles collide with the electrode surface and generate short current spikes. Naturally, the nanoparticles are rough, far from the single crystals which we consider. During the very short reaction time only the most favorable sites such as defects or edges can contribute to the reaction, so the measured rate

Fig. 4. Free energy surface for the total reaction $Zn^{++} + 2e^- \rightarrow Zn^+$ at the equilibrium potential for the total reaction.

would give an upper limit. In any case, this is an experiment which challenges our understanding of metal deposition.

4. Conclusions

In this work we have extended our model for metal deposition by including non-linear couplings between the reactant and the solvent. The free energy surfaces obtained, which are not based on any adjustable parameters, suggest a reaction path in which the first step, $Zn^{++} + e^- \rightarrow Zn^+$, takes place in an inner sphere mode and results in a physisorbed intermediate located right on the metal surface. The second electron transfer occurs on the surface and results in a Zn atom deposited on a terrace site. Our present results are a vast improvement on our previous linear theory, which predicted an outer-sphere mechanism with a prohibitively high activation energy. Direct comparison of our work with experimental data is difficult, because the latter depend strongly on the state of the surface, the effect of pH, and the nature of the anions. At least there are no experiments which contradict our work.

Finally we note that the situation for copper deposition, which we had also considered in [1] is quite different: The free energy of the Cu^+ intermediate lies only a little above that of Cu^{++}, so that an outer sphere electron transfer for the first step is quite favorable.

CRediT authorship contribution statement

Paola Quaino: Conceptualization, Methodology. **Estefania Colombo:** Investigation. **Fernanda Juarez:** Investigation. **Elizabeth Santos:** Conceptualization, Supervision, Methodology. **Gustavo Belletti:** Investigation. **Axel Groß:** Writing - review & editing, Resources. **Wolfgang Schmickler:** Conceptualization, Software, Writing - original draft.

Declaration of Competing Interest

The authors declare that they have no known competing financial interests or personal relationships that could have appeared to influence

Table 1
LJ parameters for the MD simulations.

	ϵ [kcal/mol]	σ [Å]	reference
Cu	4.72	3.166	[20]
Cu-core	3.03	2.608	provided from Sulpizi's group
dummy e^-	0.20	2.608	[20]
Zn^+ / Zn^{++}	0.00330286	2.265	[30]

Fig. 5. Energy of a Zn^+ ion approaching a Zn(0001) surface. The energy has been set to zero at large distances.

the work reported in this paper.

Appendix A. Technical details of the calculations

A.1. Molecular dynamics

Classical molecular dynamics have been carried out by using the large-scale atomic/molecular massively parallel simulator (LAMMPS) code [29]. An NTV ensemble with a temperature of 298 K was chosen.

Periodic boundary conditions have been applied in the xy directions parallel to the electrode surface. The dimensions of the simulation box were 26.25 Å $\times$ 26.25 Å $\times$ 120.91 Å. The simulation box contained an ensemble of 668 water molecules, a Cu(100) surface modeled by 6 metal layers, and a Zn^+ or Zn^{++} ion initially placed in the bulk water. For computing the long-ranged electrostatic interactions in the periodic box, the particle–particle particle-mesh (PPPM) method was used.

To evaluate the role of the image interactions, the method proposed by Geada et al. [20] has been followed, which models the induced image charge on the surface by describing every metal atom as a pair of a positive Cu core and a dummy electron of negative charge. The movement of the electrons away from the positive cores induced the polarization.

The non-covalent interactions were modeled by Coulomb and 6–12 Lennard Jones (LF) force-fields – see Table 1. The LJ parameters for the Zn^+ or Zn^{++} ions have been taken from [30]. For water we used the extended simple point charge (SPC/E) model, the corresponding parameters were described in [31]. For the LJ potential terms we applied the Lorentz-Berthelot mixing rules: $\sigma_{ij} = (\sigma_i + \sigma_j)/2$ and $\epsilon_{ij} = (\sigma_i \sigma_j)^{1/2}$. All parameters are listed in Table 1.
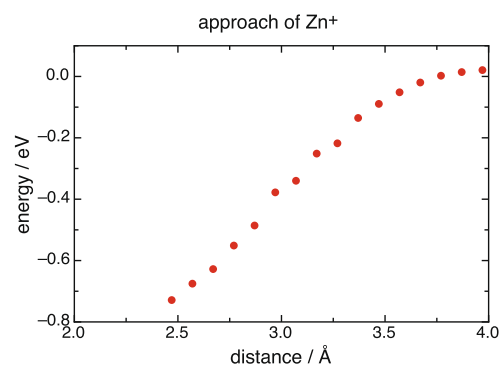
The weighted histogram analysis method (WHAM) code [32,33] was applied to obtain the potential of mean force from a series of umbrella sampling simulations. A total of 70 umbrella samplings were carried out. We started with an equilibration run of 750 ps, and then each sample ran for 250 ps with a time step of 1.0 fs.

A.2. DFT calculations

The main part of the DFT calculations have been performed with DACAPO and are detailed in [1]. Our method to obtain the coupling constants between the reactant and the electrode has been explained in [8]. Here we briefly explain how we performed the calculations for Zn^+ approaching a Zn (0001) surface. Our method has first been presented in the supporting information to the article [34], which contains the technical details of the DFT calculations. In order to generate the Zn^+ ion in DFT, we subtracted one electronic charge from the system, and applied an electric field of 2.9 V/Å

which was sufficient to localize the extra charge on the approaching ion. For this purpose it is essential to use a localized basis set, therefore we used the SIESTA code. Once the charge has been localized, one can calculate the energy of the Zn^+ ion as a function of the distance from the surface. These energy values have to be corrected both for the presence of the extra charge, which gives rise to a constant negative background charge, and the presence of the field. The corresponding theory has been developed by Lozovoi et al. [35]. Since we are not interested in the absolute values, it was sufficient to correct only for the applied field and the background charge. The resulting energy as a function of the distance for the surface is shown in Fig. 5.

References

[1] L.M.C. Pinto, P. Quaino, E. Santos, W. Schmickler, ChemPhysChem 15 (2014) 132.
[2] E. Gileadi, J. Electroanal. Chem. 660 (2011) 247.
[3] J.F. Parker, C.N. Chervin, E.S. Nelson, D.R. Rolison, J.W. Long, Energy Environ. Sci. 7 (2014) 1117.
[4] M. Jäckle, K. Helmbrecht, M. Smits, D. Stottmeister, A. Groß, Energy Environ. Sci. 2018 (11) (2018) 3400.
[5] J. Stamm, A. Varzi, A. Latz, B. Horstmann, J. Power Sources 360 (2017) 136.
[6] D. Stottmeister, A. Groß, ChemSusChem 13 (2020) 3147.
[7] W. Schmickler, E. Santos, Interfacial Electrochemistry, 2nd edition, Springer Verlag, Berlin, 2010.
[8] E. Santos, P. Quaino, W. Schmickler, PCCP 14 (2012) 11224.
[9] R.A. Marcus, J. Chem. Phys. 24 (1956) 966.
[10] R.R. Nazmutdinov, W. Schmickler, A.M. Kuznetsov, Chem. Phys. 310 (2005) 257.
[11] P.W. Anderson, Phys. Rev. 124 (1961) 41.
[12] D.M. Newns, Phys. Rev. 178 (1969) 1123.
[13] R.R. Dogonadze, A.M. Kuznetsov, J. Electroanal. Chem. 65 (1975) 545.
[14] N.S. Hush, Trans. Faraday Soc. 57 (1961) 557.
[15] W. Schmickler, Chem. Phys. Lett. 237 (1995) 152.
[16] A. Bard, R. Parsons, J. Jordan (Eds.), Standard Potentials in Aqueous Solutions, Marcel Dekker, New York, 1985.
[17] W. Schmickler, M.T.M. Koper, Electrochem. Comm. 1 (1999) 402.
[18] S.I. Pekar, Untersuchungen über die Elektronentheorie der Kristalle, Aka- demie-Verlag, Berlin, 1954, p. 184.
[19] M. Dinpajooh, M.D. Newton, D.V. Matyushov J. Chem. Phys. 146 (2017) 064504.
[20] I.L. Geada, H. Ramezani-Dakhel, T. Jamil, M. Sulpizi, H. Heinz, Nature Comm. 9 (2018) 716.

[21] M.T.M. Koper, W. Schmickler, A Unified Model for Electron and Ion Transfer Reactions on Metal Electrodes, in: Frontiers of Electrochemistry, ed. by J. Lipkowski and P.N. Ross, VCH Publishers, 1998.
[22] O. Pecina, W. Schmickler, Chem. Phys. 252 (2000) 349.
[23] S. Siahrostami, V. Tripkovic, Keld T. Lundgaard, Kristian E. Jensen, H.A. Hansen, J. S. Hummelshøj, J.S.G. Myrdal, J.K. Tejs Vegge, J. Rossmeisl Nørskov, Phys. Chem. Phys. 15 (2013) 6416.
[24] M. Sluyters-Rehbach, J.S.M.C. Breukel, J.H. Sluyters, J. Electroanal. Chem. 19 (1968) 85, and references therein.
[25] E. Eriksrud, J. Electroanal. Chem. 76 (1977) 27–49.
[26] L. Koene, M. Sluyters-Rehbach, J.H. Sluyters, J. Electroanal. Chem. 402 (1996) 57–72.
[27] G. Zampardi, R.G. Compton, J. Solid State Electrochem. 24 (2020) 2695.
[28] J. Agrisuelas, J.J. García-Jareno, D. Gimenez-Romero, F. Vicente, Electrochim. Acta 54 (2009) 6046.
[29] S. Plimpton, J. Comp. Phys. 117 (1995) 1.
[30] P. Li, P. Roberts, D.K. Chakravorty, K.M. Merz, J. Chem. Theory Comp. 9 (2013) 2733.
[31] K. Yoshida, Y. Yamaguchi, A. Kovalenko, F. Hirata, J. Phys. Chem. B 106 (2002) 5042.
[32] A.M. Ferrenberg, A.M.R.H. Swendsen, Phys. Rev. Lett 63 (1989) 1195.
[33] S. Kumar, D. Bouzida, R.H. Swendsen, P.A. Kollman, J.M. Rosenberg, J. Comput. Chem. 13 (1992) 1011.
[34] P. Quaino, N.B. Luque, R. Nazmutdinov, E. Santos, Wolfgang Schmickler, Angew. Chem. Int. Ed. 2012 (51) (2012) 12997.
[35] A. Lozovoi, A. Alavi, J. Kohanoff, R. Lynden-Bell, J. Chem. Phys. 115 (2001) 1661.